Applied Mathematical Modelling 34 (2010) 4243–4252

Contents lists available at ScienceDirect

Applied Mathematical Modelling

journal homepage: www.elsevier.com/locate/apm

Application of polynomial cellular neural networks in diagnosis of astrometric chromaticity

R. Cancelliere [a,*], M. Gai [b], A. Slavova [c]

[a] Department of Computer Science, University of Turin, 10123 Torino, Italy
[b] National Institute of Astrophysics, Astronomical Observatory of Turin, 10025 Pino Torinese (TO), Italy
[c] Institute of Mathematics and Informatics, Bulgarian Academy of Sciences, Sofia 1113, Bulgaria

ARTICLE INFO

Article history:
Received 25 February 2008
Received in revised form 21 April 2010
Accepted 28 April 2010
Available online 7 May 2010

Keywords:
Image processing
Data reduction
Lyapunov's finite majorizing equations

ABSTRACT

In this paper minimization of the chromatic error in the data reduction pipeline of the Gaia mission is presented by applying polynomial cellular neural networks (PCNN). We introduce generalized PCNN model which enables us to solve the nonlinear approximation task. The advantage of the newly proposed method is in solving large-size image processing problem of diagnosis of astrometric chromaticity in real time. Rigorous stability analysis of the PCNN is presented by using the method of Lyapunov's finite majorizing equations. The simulation results show a linear relation between the output of the proposed PCNN model and the chromaticity values as the target data.

1. Introduction

When the photometric signal to noise ratio (*SNR*) is sufficiently high the location of the position of a stellar image is possible with uncertainty well below its characteristic size.

The best estimate of image position is obtained evaluating the discrepancy between the data and the template describing the reference image using a least square method, so the location algorithm is very sensitive to any variation of the actual image with respect to the selected template.

Some important aspects are the possibility to check the compatibility between the real image and the reference profile and also the capability of extracting from the data a set of parameters suitable for a new definition of the template, in order to improve its consistency with the data. Self-calibration of the data, by deduction of the parameters for optimisation of the image template, is a key element in the control of the systematic effects in the position measurement.

The issue of astrometric errors induced by the variation of spectral distribution among stars, i.e. chromaticity, and its treatment, is discussed e.g. for the Hipparcos mission in Pourbaix [1]; another interesting use of neural networks for spectral analysis can be found in [2], while in [3] sigmoidal neural network is used for diagnosis and correction of the chromaticity in the framework of the astrometric mission Gaia [4].

In this paper we study a new neural network architecture, i.e. polynomial cellular neural network (PCNN) for solving the above problem. Our choice is due to the existence of different works concerning the use of neural networks in astronomical adaptive optics (see [5,6]) where they always demonstrated great robustness to noise and damages and powerful capabilities of flexible learning.

Cellular neural networks (CNN, [7,8]), introduced by Chua and Yang in 1988, have the basic application in image processing. They are novel class of information processing systems constructed as an analog dynamic processor array which reflects

* Corresponding author. Tel.: +39 0116706777; fax: +39 011751603.
E-mail address: cancelli@di.unito.it (R. Cancelliere).

0307-904X/$ - see front matter © 2010 Elsevier Inc. All rights reserved.
doi:10.1016/j.apm.2010.04.021

just this property: the processing elements interact directly within a finite local neighborhood. In the image processing tasks CNN use parallel processing of the input image space and delivers its output in continuous time. This remarkable feature makes it possible to process a large-size image in real time. For this reason the idea is to apply PCNN in order to minimize the chromatic errors in the data reduction pipeline of the Gaia mission. We consider a CNN programmable realization allowing the calculation of all necessary processing steps in real time.

In recent investigations Reaction Diffusion Cellular Nonlinear Networks (RD-CNN) with polynomial weight functions have been applied for modeling complex systems – like the Fitzhugh–Nagumo, Lotka–Volterra system with high accuracy [9,10]. PCNN may reveal possible, inherent changes in brain dynamics which lead to ictal onsets and represent a novel approach to information processing with CNN [11]. In different approaches to the feature extraction problem nonlinear CNN with polynomial weight functions have been used [12] especially for the signal prediction. Moreover, an increase of the polynomial order leads to better convergence and improved accuracy of the used optimization algorithm.

In Section 2 we briefly describe the astronomical problem and the image encoding technique, in Section 3 we resume the main features of CNN and PCNN, in Section 4 we introduce generalized PCNN, in Section 5 we prove absolute global asymptotic stability of generalized PCNN and in Section 6 we describe the current results.

2. Diffraction imaging

For an unobstructed circular pupil of diameter D, at wavelength λ, the image of a star, considered as a point-like source at infinity, and produced by an ideal telescope, has radial symmetry and is described by the squared Airy function (2.1) (see [13] for notation)

$$I(r) = k[2J_1(v)\}/v]^2, \quad v = \pi r D/\lambda F. \tag{2.1}$$

J_1 is the Bessel function of the first kind, order one, k a normalisation constant, and r is the radial coordinate on focal plane.

The diffraction image on the focal plane of *any* real telescope, described by a set of aberration values, for a given pupil geometry, is deduced by the square modulus of the Fourier transform of the pupil function $e^{i\Phi}$:

$$I(r,\varphi) = \frac{k}{\pi^2}\left|\int d\rho \int d\theta \rho e^{i\Phi(\rho,\theta)} e^{-i\pi r\rho\cos(\theta-\phi)}\right|^2, \tag{2.2}$$

where $\{r,\phi\}$ and $\{\rho,\theta\}$ are the radial coordinates, respectively on image and pupil plane, and the integration domain corresponds to the pupil (for the circular case, $0 \leqslant \rho \leqslant 1$ and $0 \leqslant \theta \leqslant 2\pi$).

The phase aberration Φ describes the wavefront error (WFE) i.e. in a real case the deviation from the ideal flat wavefront and can be decomposed by means of the first 21 terms of the Zernike functions (as described in [13]):

$$\Phi(\rho,\theta) = \frac{2\pi}{\lambda} WFE = \frac{2\pi}{\lambda}\sum_{n=1}^{21} A_n \phi_n(\rho,\theta). \tag{2.3}$$

If $\Phi = 0$ (non-aberrated case, $\{A_n\} = 0$), we obtain a flat wavefront, i.e. $WFE = 0$, and Eq. (2.1) is retrieved for the circular pupil.

The nonlinear relation between the set of aberration coefficients A_n and the image is evident by replacement of Eq. (2.3) in Eq. (2.2).

The real polychromatic image of an unresolved stellar source is produced by integration of the monochromatic PSF above over the appropriate bandwidth, weighed by the combination of source spectral distribution, instrument transmission and detector response. Thus, objects with different spectral distributions have different image profiles, and the position estimate produced by any location algorithm (e.g. the centre of gravity, COG, or barycentre) is affected by discrepancy with respect to the nominal position from the image generated by an ideal optical system.

The variation of apparent position with source spectral distribution is what we call chromaticity, and it is relevant to high precision astrometry. Not all aberrations are relevant to chromaticity, but the relationship is not mathematically trivial; the critical terms introduce an asymmetry in the image, along the measurement direction, and are associated to odd parity functions. An analysis of chromaticity *versus* aberrations, optical design aspects, and optical engineering issues, are discussed in [14], which also deals with design optimization guidelines. After minimization of the chromaticity by design and construction, the residual chromaticity must be taken into account in the data reduction phase.

In the current paper we are interested in investigating the capability of a PCNN to implement identification of the chromatic effect from the image profile itself.

The chromaticity is estimated as difference between the COG of a blue (B3V) and red (M8V) stars, modeled as black bodies, with effective wavelengths 628 nm and 756 nm respectively, deduced by taking into account also the telescope transmission and detector quantum efficiency. A set of aberration cases is generated for the basic telescope geometry of Gaia under the assumption of small image degradation, i.e. of reasonably good imaging performance, as desired for large field astronomical telescopes. The aberration coefficients are generated with a uniform random distribution with peak value 50 nm for each component, using the Zernike formulation. The coefficient range is not specific of a given configuration, but represents all mathematically possible cases, i.e. a superset of the optically feasible systems.

2.1. Image encoding

To maximize the field of view, i.e. observe simultaneously a large area, typical astronomical images are sampled over a small number of pixels.

The minimum sampling requirements, related to the Nyquist–Shannon criterion, are of order of two pixels over the full width at half maximum, or about five pixels within the central diffraction peak. The signal detected in each pixel is then affected by strong variations depending on the initial phase (or relative position) of the parent intensity distribution (the continuous image) with respect to the pixel array, even in a noiseless case. The pixel intensity distribution of the measured images, then, is not convenient for evaluating the discrepancy of the effective image with respect to the nominal image.

It is possible to provide good sampling for the images in small region: in this case, the resolution is adequate to minimize the effects of the finite pixel size. But in Gaia this would have an heavy impact on the payload. If we use a neural network with input data for the image size $60 \times 60 = 3600$ pixels, then a large computational load is involved.

Since the Gaia measurement is one-dimensional, and most images are integrated in the across scan direction, the problem (and the signals considered) is also reduced to one-dimension, conventionally labeled y: the one-dimensional image is $I(y)$. The encoding scheme we adopt for the images allows extraction of the desired information for classification; each input image is described by the center of gravity and the first central moments as follow:

$$\begin{aligned} \mu_y &= \int dy\, y \cdot I(y)/I_{int}, \\ \sigma_y^2 &= \int dy (y-\mu_y)^2 \cdot I(y)/I_{int}, \\ M(j) &= \int dy \left(\frac{y-\mu_y}{\sigma_y}\right)^j \cdot I(y)/I_{int}, \quad j > 2, \end{aligned} \tag{2.4}$$

where $I_{int} = \int dy I(y)$ is the integrated photometric level of the measurement over an opportune finite image domain.

One-dimensional encoding is a further change with respect to previous problems, in which we took advantage of the full two-dimensional image structure to deduce the different aberration terms.

The central moments are much less sensitive than the pixel intensity values to the effects related to the finite pixel size and the position of the image peak with respect to the pixel borders, i.e. the relative phase between optical image and pixel array. Thus, central moments can be deduced conveniently also on the detected low resolution images, without the need for high resolution detectors. The encoding technique based on using moments as image description parameters for neural processing was first introduced in [15], where more details are available.

We are interested in the classification capability of a polynomial CNN in the case of small image perturbations, i.e. of reasonably good image quality, as desired for large field astronomical telescopes.

3. Polynomial cellular neural networks

Cellular Neural Networks (CNNs) are complex nonlinear dynamical systems. CNN (see [7]) is simply an analogue dynamic processor array, made of cells, which contain linear capacitors, linear resistors, linear and nonlinear controlled sources. Let us consider a two-dimensional grid with 3×3 neighborhood system as it is shown on Fig. 1.

The squares are the circuit units-cells, and the links between the cells indicate that there are interactions between linked cells. One of the key features of a CNN is that the individual cells are nonlinear dynamical systems, but that the coupling between them is linear. Roughly speaking, one could say that these arrays are nonlinear but have a linear spatial structure, which makes the use of techniques for their investigation common in engineering or physics attractive.

We will give the general definition of a CNN which follows the original one [7]:

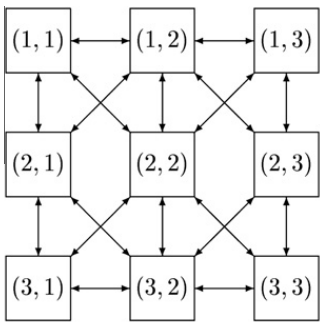

Fig. 1. One-layer two-dimensional CNN.

$$x(t) = \widetilde{L}_1\widetilde{F}_1(x,\eta,t,u), \qquad (5.21)$$
$$\eta(t) = \widetilde{L}_2\widetilde{F}_2(x,\eta,t,u).$$

It is easy to see that the operators $\widetilde{L}_1$ and $\widetilde{L}_2$ are linear, bounded and therefore continuous.

Now we construct the following system of Lyapunov's majorizing equations in the certain domain $u \in [0, u^*]$:

$$\alpha(u) = \tilde{\rho}_1\Phi(\alpha,\beta,u),$$
$$\beta(u) = \tilde{\rho}_2\Psi(\alpha,\beta,u), \qquad (5.22)$$

where $\Phi(\alpha,\beta,u)$ and $\Psi(\alpha,\beta,u)$ are Lyapunov's majorants for $\widetilde{F}_1$ and $\widetilde{F}_2$, respectively. Moreover, $\alpha \geqslant |x|$ and $\beta \geqslant |\eta|$.

Therefore according to the properties of Lyapunov's majorizing equations [17,18] the following theorem has been proved:

Theorem 1. *Suppose that system (5.22) in the domains $t \in [0,T]$ and $u \in [0,u^*]$ has positive solutions $\alpha = \alpha(u)$ and $\beta = \beta(u)$ for $0 \leqslant u \leqslant u^*$ and $\|\alpha(u^*)\| \leqslant const.$, $\|\beta(u^*)\| \leqslant const.$. Then system (5.15) has for $u \in [0,u^*]$ solutions $x(t,u)$, $\eta(t,u)$, which are unique in the classes of functions $C[t]$ and $C[u]$. These solutions can be found by the following convergent simple iterations:*

$$x_s = \widetilde{L}_1\widetilde{F}_1(x_{s-1},\eta_{s-1},t,u), \qquad (5.23)$$
$$\eta_s = \widetilde{L}_2\widetilde{F}_2(x_{s-1},\eta_{s-1},t,u), \quad s = 1,2,\ldots,$$
$$x_0 \equiv x(0), \quad \eta_0 \equiv \eta(0).$$

Remark 1. Using the method of Lyapunov's majorizing equations is a new approach in studying the stability of CNN. Moreover, we find the stable equilibrium states of our CNN with the help of the simple iterations (x_s, η_s) by fixing $u = u^*$ and $t = t_0$.

In this sense Theorem 1 proves that after the transient has decayed to zero in the circuit, CNN always settle at the stable equilibrium states x^* and η^* given by the following formulas:

$$x^* = \widetilde{L}_1\widetilde{F}_1(x^*,\eta^*,u^*,t_0),$$
$$\eta^* = \widetilde{L}_2\widetilde{F}_2(x^*,\eta^*,u^*,t_0). \qquad (5.24)$$

Remark 2. It is easily to prove that the output $y(t) = \frac{1}{1+e^{-\eta}}$ is a constant after the transient has decayed to zero in the circuit. In other words we have:

$$\lim_{t\to\infty} y(t) = \text{const.} \qquad (5.25)$$

We will prove now the global asymptotic stability of our polynomial GCNN. We defined the equilibrium states by (5.24) and according to the Theorem 1 they are the unique equilibrium states of the system. Therefore following the Definition 4 we will prove global asymptotic stability of polynomial GCNN described by (4.9)–(4.12):

Theorem 2. *Consider the variables associated with a single cell in a polynomial network of many cells described by the dynamical system* 4.9, 4.10, 4.11, 4.12 . Suppose that the output nonlinearity $f(.)$ is Lipschitz continuous and A is negative. Under these conditions, for each constant input $u = u^*$ the cell has a globally asymptotically stable equilibrium points (x^*, η^*), which are the unique solutions of 4.9, 4.10, 4.11, 4.12 *if the following conditions are satisfied:*

(i) $|x(0)| \leqslant 1$, $|\eta(0)| \leqslant 1$, $|u| \leqslant 1$;
(ii) system of Lyapunov's majorizing Eq. (5.22) has positive solutions and the following estimates are satisfied:

$$\|x(u,t)\| \leqslant \alpha(u),$$
$$\|\eta(u,t)\| \leqslant \beta(u).$$

Such stability is called absolute global stability.

Proof. Given a cell with constant input, let us derive another cell with zero input such that an equilibrium point x_i^* of the given cell is globally asymptotically stable if and only if the equilibrium point *0* of the new cell is globally asymptotically stable. Let $((x^*)^T, \eta^*)^T$ be a solution of (5.24). By a change of variables, the dynamical system of Eqs. (4.9)–(4.12) can be transformed into the system:

$$\dot{\bar{x}}(t) = A\bar{x}(t) + B\bar{v}(t), \qquad (5.26)$$
$$\bar{\eta}(t) = C^T\bar{x}(t) + D\bar{v}(t), \qquad (5.27)$$
$$\bar{y}(t) = G(\bar{\eta}(t)) = f(\bar{\eta}(t) + \eta^*) - f(\eta^*), \qquad (5.28)$$

where $\bar{x}(t) = x(t) - x^*$, $\bar{v}(t) = v(t) - v^*$, $\bar{y}(t) = y(t) - y^*$, $\bar{\eta}(t) = \eta(t) - \eta^*$, $y^* = f(\eta^*)$.

6. Simulations and obtained results

In this section we will apply polynomial CNN approach to the problem of detection of astrometric chromaticity. The network parameter values of a multi-layer CNN with polynomial cell coupling, described by the dynamical system (4.9)–(4.12), are determined in a supervised optimization process (see Fig. 3). In our specific case of simulation we take the number of the layers of the GPCNN $m = 3$ and on each layer we have a grid with 100 cells.

The coefficients $b_{ll'}^{(k)}$ can be determined if the inner structure of a system is unknown in a supervised optimization process [9]. Thereby the Taylor approximation of the output function (4.11) in Fig. 4 was used as reference.

During the optimization process the mean square error

$$e_{mse} = \sum_t \sum_j \sum_{l=1}^{m} \frac{\left(y_j^l - \tilde{y}_j^l\right)^2}{N} \tag{6.32}$$

is minimized using Powell method and Simulated Annealing [12]. In each step e_{mse} is calculated by taking the reference $y_j^l(t)$ of the target and the output $\tilde{y}_j^l$ of a polynomial CNN obtained by the CNN simulation system MATCNN applying 4th order

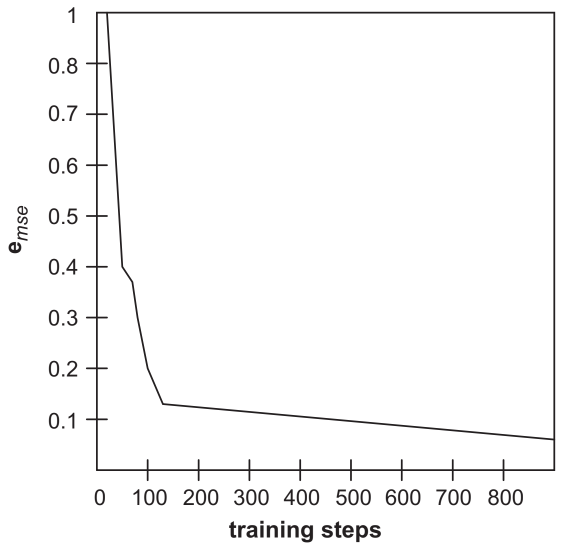

Fig. 5. Minimization of the mean square error e_{mse} during the parameter optimization process.

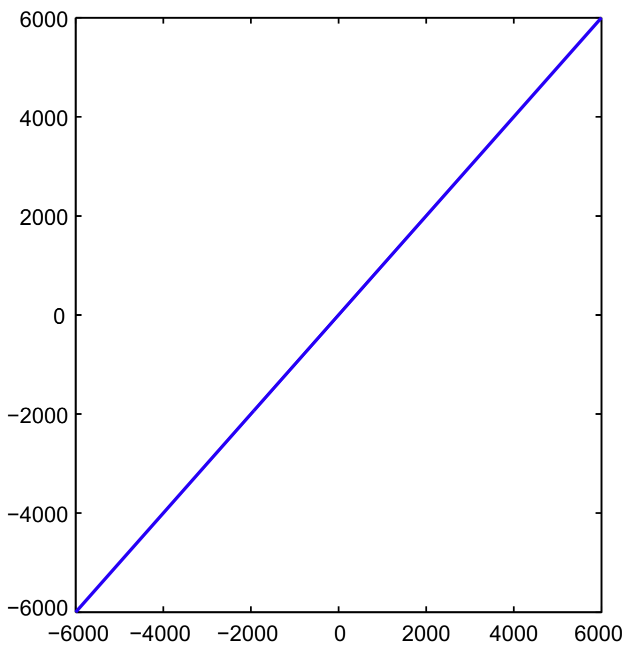

Fig. 6. Target $y_j^l(t)$ (x-axis) – Output $\tilde{y}_j^l$ (y-axis) results of the simulation.

Runge–Kutta integration (see Fig. 3). Fig. 5 shows the decreasing mean square error e_{mse} during the optimization process; only errors with $e_{mse}(h) < e_{mse}(h-1)$ for training steps h are given.

Fig. 6 shows the solutions of the polynomial CNN determined in an optimization process, by using the reference pattern shown in Fig. 4. Obviously, we obtain that the relation between polynomial network ouputs and target values is very close to a linear case.

Remark 4. In [3] a sigmoidal neural network with a hidden layer with 300 internal nodes, trained on a set of 20,000 data instances and evaluated on a test set of 5820 cases, is applied for diagnosis and correction of the chromaticity. In the present work we introduce new architecture – polynomial cellular neural networks with 3 layers in our simulation for the same problem. The difference here is that the nonlinear coupling between layers and cell feedback is of polynomial type with coefficients which have to be determined in an optimization process. For this purpose we calculate the mean square error e_{mse} which is minimized and on Fig. 5 the decreasing e_{mse} is shown during the optimization process of 800 training steps. In order to minimize the computational complexity and to maximize the significance of the mean square error we take 100 cells on each layer of our PCNN.

7. Conclusions

In this paper we apply PCNN for minimization of the chromatic error in the data reduction pipeline of the Gaia mission. Moreover, we introduce generalized PCNN which is a very good model for a broad class of non-linearities. CNN with polynomial weight functions has advantages because the essential information can be extracted from the data, in our case the chromaticity values, without topographically arranged data units. The proposed generalized PCNN model can be used for solving large-size image processing problems in real time.

Rigorous analysis of the stability of such network model is presented by applying the method of Lyapunov's finite majorizing equations. In Theorem 2 we prove absolute global asymptotic stability of the PCNN model. Simulations based on 4th order Runge–Kutta integration are made and we obtain linear relation between PCNN outputs and target data, i.e. the chromaticity values (see Fig. 6).

References

[1] D. Pourbaix, Chromatic effects in Hipparcos parallaxes and implications for distance scale, in: IAU Colloqium 196: D.W. Kurtz (Ed.), Transits of Venus: New Views of the Solar System and Galaxy, 2005, pp. 377–385.
[2] M. Bazarghan, R. Gupta, Automated classification of sloan digital sky survey (SDSS) stellar spectra using artificial neural networks, Astrophys. Space Sci. 315 (2008) 201–210.
[3] M. Gai, R. Cancelliere, Neural network correction of astrometric chromaticity, Mon. Not. R. Astron. Soc. 362 (4) (2005) 1483–1488.
[4] M.A.C. Perryman et al., GAIA – composition, formation and evolution of the galaxy, Concept and technology study, Report and Execution, Summary, ESA-SCI ,vol. 4, European Space Agency, Munich, Germany, 2000.
[5] M. Loyd-Hart, P. Wizinowich, B. McLeod, D. Wittman, D. Colucci, R. Dekany, D. McCarthy, J.R.P. Angel, D. Sandler, First results of an on-line adaptive optics system with atmospheric wavefront sensing by an artificial neural network, Astrophys. J. 390 (1992) L41–44.
[6] P. Wizinowich, M. Loyd-Hart, R. Angel, Adaptive optics for array telescopes using neural networks techniques on transputers, Transputing '91, 1, IOS Press, Washington D.C, 1991, pp. 170–183.
[7] L.O. Chua, L. Yang, CNN: Theory, IEEE Trans. Circuits Syst. 35 (1988) 1257–1272.
[8] L.O. Chua, L. Yang, CNN: applications, IEEE Trans. Circuits Syst. 35 (1988) 1273–1299.
[9] A. Slavova, M. Markova, Polynomial Lotka–Volterra CNN model: dynamics and complexity, C.R. Acad. Sci. Bulg. 60 (12) (2007) 1271–1276.
[10] A. Slavova, P. Zecca, Complex behaviour of polynomial FitzHugh–Nagumo CNN model, Nonlinear Anal. Real World Appl. 8 (4) (2007) 1331–1340.
[11] M.Laiho, A.Paasio, K.Halonen, Structure of a CNN with linear and second order polynomial feedback terms, in: Proceedings of IEEE CNNA'2000, Catania, 2000, pp. 401–406.
[12] R. Tetzlaff, F. Gollas, Modeling complex systems by reaction–diffusion cellular nonlinear networks with polynomial weight-functions, in: Proceedings of IEEE CNNA, 2005.
[13] M. Born, E. Wolf, Principles of Optics, Pergamon, New York, 1985.
[14] M. Gai, D. Busonero, D. Loreggia, D. Gardiol, M.G. Lattanzi, Chromaticity in all-reflective telescopes for astrometry, Astron. Astrophys. (2004).
[15] R. Cancelliere, M. Gai, A comparative analysis of neural network performances in astronomy imaging, Appl. Numer. Math. 45 (1) (2003) 87–98.
[16] R. Cancelliere, A. Slavova, Dynamics and stability of generalizded cellular neural network model, Appl. Math. Comp. 165 (1) (2005) 127–136.
[17] E.A. Grebenikov, Yu.A. Ryabov, Constructive Methods in the Analysis of Nonlinear Systems, Mir Publisher, Moscow, 1979. English translation.
[18] A.M. Lyapunov, General Problem about the Stability of Motion, Gostekhizdat, Moscow, Russia, 1950.